Steady State Analysis of Quadratic Boost and Interleaved Boost Converters for Renewable Energy Applications- A Comparative Study

C. Naga Kota Reddy[1], Ch. Sai Babu[2]
[1] Research Scholar, Department of EEE,
University College of Engineering Kakinada (A), JNTU Kakinada,
Kakinada, India
[2] Professor, Department of EEE,
University College of Engineering Kakinada (A), JNTU Kakinada,
Kakinada, India

***Abstract*—** Recently, renewable energy sources have acquired more attention as compared with conventional energy sources due of their renewable and eco-friendly nature. DC-DC converters are crucial in their applications. Two different configurations based on the conventional boost converter are compared for renewable energy source applications in this paper. In one configuration, two boost converters are connected in series with a single switch (Quadratic Boost Converter), and in another, they are connected in parallel with two switches (Interleaved Boost Converter). The first configuration has a high voltage gain with a low duty cycle, while the second has a low input current ripple. The two configurations are compared in various aspects, like output voltage, voltage gain, inductor current, inductor current ripple and component counts. The configurations are designed in the MATLAB simulation environment by using the PLECS block set to validate the theoretical studies with ideal values. With a duty cycle value of 0.6 and a 12 V input voltage, the output voltage of the quadratic boost converter is 75 V and that of the interleaved boost converter is 30 V.

***Index Terms*— Boost Converter, Quadratic Boost Converter, Interleaved Boost Converter, Output voltage, Voltage Gain, Inductor Current Ripples.**

I. INTRODUCTION

As a result of the shortage of fossil fuels and the production of greenhouse gases, sustainable energy sources (i.e. solar, fuel cells and wind) have attained more attention. In addition to the above, renewable energy sources also help in the generation of electrical power at demand sites, adaptability and credibility [1]. The sustainable energy sources produce a variable and low output voltage, which demands a DC-DC boost converter with high voltage gain [2-3]. In many of the modern applications, a high voltage gain DC-DC converters are more desirable. High voltage gain DC-DC converters have a variety of uses, such as in automotive HID light ballasts, DC microgrids, and computer server power supplies for the telecommunications sector. One of the applications of high voltage gain DC-DC converter is depicted in Fig.1 [4]. To step up the low voltage of sustainable energy sources typically DC-DC Boost converters are used. These converters are frequently classified into two categories: non-isolated and isolated. There seems to be an electrical common link between the outputs and inputs in non-isolated converters.

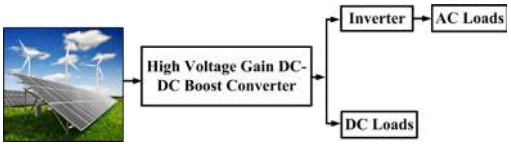

Fig. 1. A High Voltage Gain DC-DC converter used in renewable energy source applications.

These also are uncomplicated to put into practice in practical systems and prototypes because they only use basic components such as switches, diodes, inductors, and capacitors. The name suggests the existence of no shared link between the output and the input, which can be accomplished using transformer in isolated converters. Owing to the discontinuous input current, such converters are not suitable for renewable energy applications and, in addition, increase the price, complexity and design are heavy [5-8]. As shown in Fig. 2, the standard Boost Converter (BC) is generally used to increase the DC voltage when it is required.

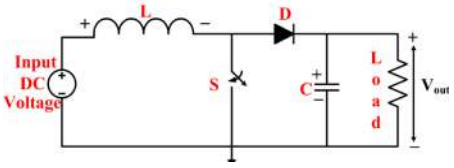

Fig. 2. Topology of boost converter

In BC, a huge value of duty cycle is preferred to achieve a large voltage gain. But increases in losses have reduced efficiency [9]. Without the use of a large value duty cycle, series connection of two BCs provides enhanced voltage gain [10] and is shown in Fig.3. As illustrated in Fig. 4, the structure of a QBC is developed from a two-stage cascading boost converter with only a

single active switch [11-12]. The QBC consists of two inductors (L1 and L2), two capacitors (C1 and C2), three diodes (D1, D2 and D3), a switch (S), a load (R), and an input DC voltage source (Vin). The QBC's voltage gain has been enhanced, as has the converter's switch voltage stress [13].

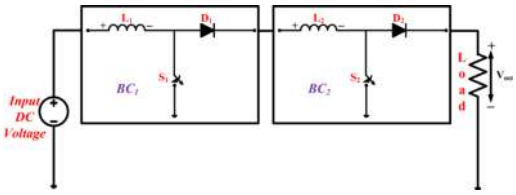

Fig. 3. Series Connection of BCs

The parallel connection of two BC's is depicted in Fig.5 it provides reduced ripple in the input current. Many benefits over the BC may be found in the Interleaved Boost Converter (IBC), such as minimal switching loss, improved efficiency, and so on [14-15]. The topology of IBC is depicted in Fig. 6. The IBC consists of two inductors (L1 and L2), a capacitor (C), two diodes (D1 and D2), two switches (S1 and S2), a load (R), and an input DC voltage source (V*in*).The coupled inductors are used in applications requiring high power and performance [16-17]. The voltage gain of IBC can be extended using voltage multipliers [18]. All the components used in the circuits have their standard meaning.

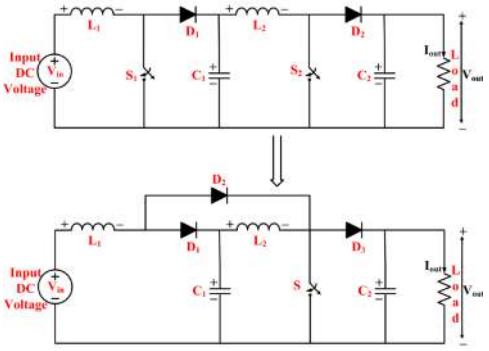

Fig.4 Topology of Quadratic Boost Converter

The goal of this study is to provide a comparative perspective on the steady state analysis of two converters. Section 2 examines the operation and steady-state analysis of QBC including the requisite equations, output voltage and voltage gain. Analyse the operation of IBC in steady state in section 3. Section 4 describes the simulation results and their discussions, and also provides a comparison between QBC and IBC for the same specifications. Section 5 gives the conclusion. The analysis is carried out on the assumption that all of the components are ideal and also that the capacitors are sufficiently stiff throughout operation [19].

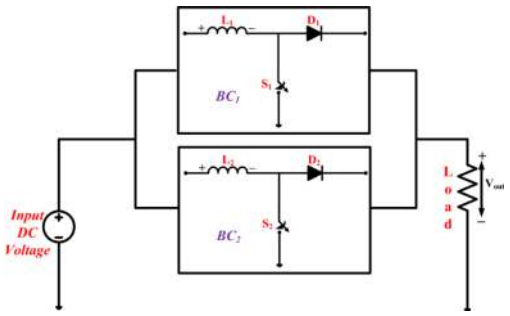

Fig.5. Parallel Connection of BCs

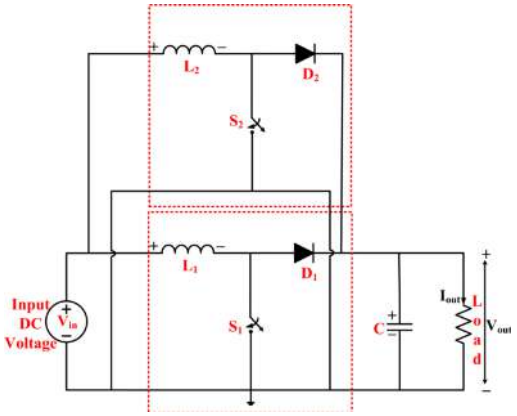

Fig.6. Topology of Interleaved Boost Converter

II. Operation and Steady State Analysis of QBC

Switching pulse for QBC is indicated in Fig. 7. Over the switching period (T_s), the switch (S) is on during δT_s and off during $(1–\delta)T_s$. where δ gives the duty cycle. During δT_s, the switch is on, when the switch is on, L_1 and L_2 are charged by V_{in} and V_{C1} (voltage across C_1), respectively. C_1 and C_2 discharge their energy to L_1 and the load, respectively. The current of L_1 (I_{L1}), Current of L_2 (I_{L2}) and output current (I_{out}) are indicated depicted circuit of QBC in Fig. 8(a). When the switch is off during $(1–\delta)T_s$, L_1 discharges to C_1 and L_2 discharges to C_2 and load. Fig. 8(b) indicates the circuit of QBC when the switch is off during $(1–\delta)T_s$.

The voltage across L_1 during δT_s and $(1–\delta)T_s$ are written as

$$\langle v_{L1} \rangle_{on} = V_{in} \qquad \text{(Eq.1)}$$

$$\langle v_{L1} \rangle_{off} = V_{in} - V_{C1} \qquad \text{(Eq.2)}$$

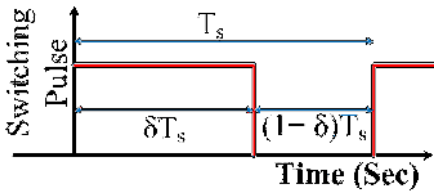

Fig.7. Switching pulse for QBC

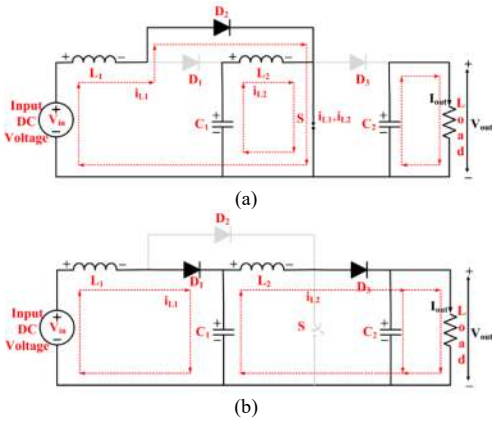

Fig.8. QBC circuit during (a) δTs (i.e. S is on) and (b) (1–δ)Ts (i.e. S is off)

The voltage across L_2 during δT_s and $(1-\delta)T_s$ are written as

$$\langle v_{L2}\rangle_{on} = V_{C1} \quad \text{(Eq.3)}$$

$$\langle v_{L2}\rangle_{off} = V_{C1} - V_{out} \quad \text{(Eq.4)}$$

The current flowing through C_1 (i_{C1}) during δT_s and $(1-\delta)T_s$ are written as

$$\langle i_{C1}\rangle_{on} = -I_{L2} \quad \text{(Eq.5)}$$

$$\langle i_{C1}\rangle_{off} = I_{L1} - I_{L2} \quad \text{(Eq.6)}$$

The current flowing through C_2 (i_{C2}) during δT_s and $(1-\delta)T_s$ are written as

$$\langle i_{C2}\rangle_{on} = -I_{out} \quad \text{(Eq.7)}$$

$$\langle i_{C1}\rangle_{off} = I_{L2} - I_{out} \quad \text{(Eq.8)}$$

By applying volt–sec balance at L_1, the voltage across capacitor C_1 (V_{C1}) is obtained as

$$V_{C1} = \frac{V_{in}}{1-\delta} \quad \text{(Eq.9)}$$

By applying volt–sec balance at L_2, the voltage across capacitor C_2 ($V_{C2} = V_{out}$, Output voltage) is obtained as

$$V_{C2} = V_{out} = \frac{V_{in}}{(1-\delta)^2} \quad \text{(Eq.10)}$$

The voltage gain of the QBC is written as

$$G = \frac{V_{out}}{V_{in}} = \frac{1}{(1-\delta)^2} \quad \text{(Eq.11)}$$

By applying amp–sec balance at C_1, the current flowing through L_1 (I_{L1}) is obtained as

$$I_{L1} = \frac{I_{out}}{(1-\delta)^2} = \frac{V_{in}}{(1-\delta)^4 R} \quad \text{(Eq.12)}$$

By applying amp–sec balance at C_2, the current flowing through L_2 (I_{L2}) is obtained as

$$I_{L2} = \frac{I_{out}}{(1-\delta)} = \frac{V_{in}}{(1-\delta)^3 R} \quad \text{(Eq.13)}$$

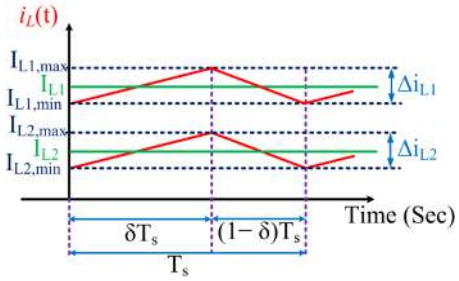

Fig.9. Inductor Currents of L_1 and L_2

The currents I_{L1} and I_{L2} are varying between maximum and minimum values a ripple of Δi_{L1} and Δi_{L2} respectively and are shown in the Fig. 9. The maximum ($I_{L1,\ max}$) and minimum ($I_{L1,\ min}$) currents of I_{L1} are obtained as

$$I_{L1,\max} = V_{in}\left[\frac{1}{(1-\delta)^4 R} + \frac{\delta}{2L_1 f_s}\right] \quad \text{(Eq.14)}$$

$$I_{L1,\min} = V_{in}\left[\frac{1}{(1-\delta)^4 R} - \frac{\delta}{2L_1 f_s}\right] \quad \text{(Eq.15)}$$

The maximum ($I_{L2,\ max}$) and minimum ($I_{L2,\ min}$) currents of I_{L2} are obtained as

$$I_{L2,\max} = V_{in}\left[\frac{1}{(1-\delta)^3 R} + \frac{\delta}{2(1-\delta)L_2 f_s}\right] \quad \text{(Eq.16)}$$

$$I_{L2,\min} = V_{in}\left[\frac{1}{(1-\delta)^3 R} - \frac{\delta}{2(1-\delta)L_2 f_s}\right] \quad \text{(Eq.17)}$$

The critical value of the inductor (L_{cri}) is essential for Continuous Conduction Mode (CCM) of operation of the converter. By equating $I_{L1,\ min}$ and $I_{L2,\ min}$ to zero, as the inductors' L_1 and L_2 critical values are

$$L_{1,cri} = \frac{(1-\delta)^4 \delta R}{2 f_s} \quad \text{(Eq.18)}$$

$$L_{2,cri} = \frac{(1-\delta)^2 \delta R}{2 f_s} \quad \text{(Eq.19)}$$

III. Operation and Steady State Analysis of IBC

The switching pulses for IBC have a 180° phase shift and are depicted in Fig.10. The IBC may operate in three different modes if the duty cycle is greater than 0.5 [20-22]. S_1 and S_2 have on and off times denoted by δT_s and by $(1-\delta)T_s$, respectively. During mode-I, both of the

S_1 and S_2 are on. In mode II, S_1 is on and S_2 is off. S_1 is off, while S_2 is on in mode-III. Fig. 10 depicts the IBC's functioning in three different modes.

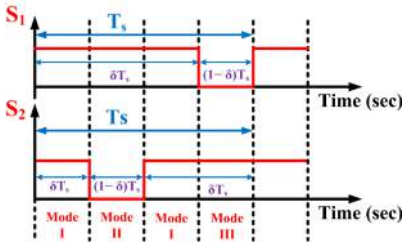

Fig.10. Switching pulses for IBC

The circuit is shown in mode-I in Fig. 11(a), with V_{in} charging L_1 and L_2 and C discharging to the load. L_1 is charged by V_{in} in mode II, and L_2 discharges to the C and load, as shown in Fig. 11(b). The mode-III circuit is shown in Fig. 11(c), where L_2 is charged by V_{in} and L_1 discharged to C and the load.

The voltage across L_1 (V_{L1}) during the on and off of S_1 is written as

$$\langle v_{L1} \rangle_{on} = V_{in} \qquad \text{(Eq.20)}$$

$$\langle v_{L1} \rangle_{off} = V_{in} - V_{out} \qquad \text{(Eq.21)}$$

The voltage across L_2 (V_{L2}) during the on and off of S_2 is written as

$$\langle v_{L2} \rangle_{on} = V_{in} \qquad \text{(Eq.22)}$$

$$\langle v_{L2} \rangle_{off} = V_{in} - V_{out} \qquad \text{(Eq.23)}$$

The charging current of C, when S_1 is off is written as

$$\langle i_C \rangle = I_{L1} - I_{out} \qquad \text{(Eq.24)}$$

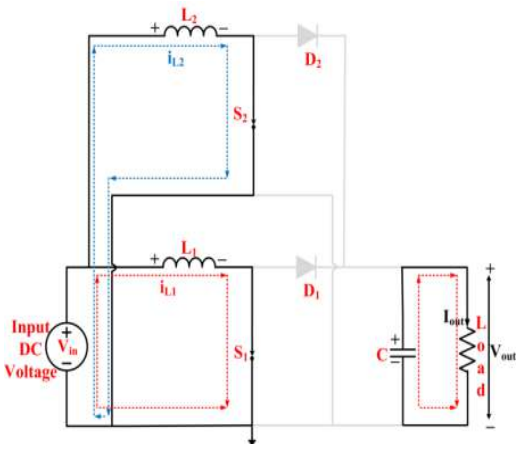

(a)

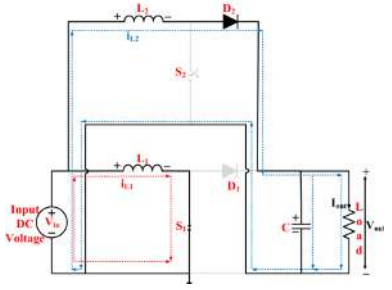

(b)

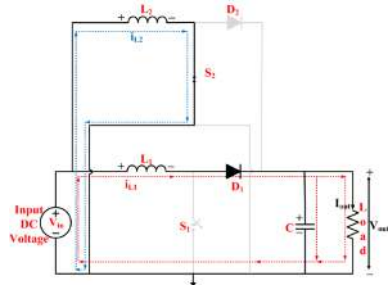

(c)

Fig.11. IBC circuit during (a) S_1 and S_2 are on, (b) S_1 is on and S_2 is off and (c) S_1 is off and S_2 is on

The charging current of C, when S_2 is off is written as

$$\langle i_C \rangle = I_{L2} - I_{out} \qquad \text{(Eq.25)}$$

The discharging current of C is written as

$$\langle i_C \rangle = -I_{out} \qquad \text{(Eq.26)}$$

By applying volt–sec balance at either L_1 or L_2, the output voltage (V_{out}) is obtained as

$$V_{out} = \frac{V_{in}}{1-\delta} \qquad \text{(Eq.27)}$$

The output voltage comparison between QBC and IBC is drawn for the constant V_{in} is shown in Fig. 12. It demonstrates that for a given V_{in} and δ, QBC has a higher value than IBC. The difference grows larger as δ increases.

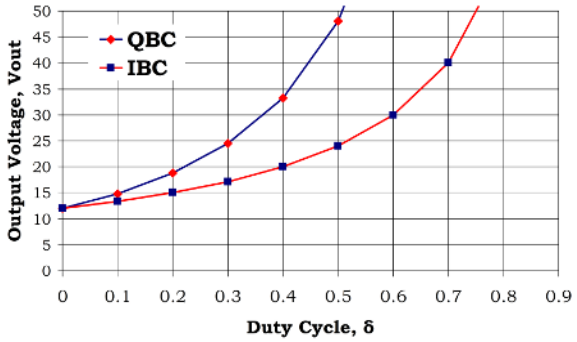

Fig. 12. Comparison of output voltages with constant Vin between QBC and IBC

The IBC's voltage gain is achieved as

$$G = \frac{V_{out}}{V_{in}} = \frac{1}{1-\delta} \qquad \text{(Eq.28)}$$

The variation in voltage gain for various duty cycle values is appeared in Fig.13 for IBC and QBC. The voltage gain distinction between IBC and QBC increases for a given duty cycle.

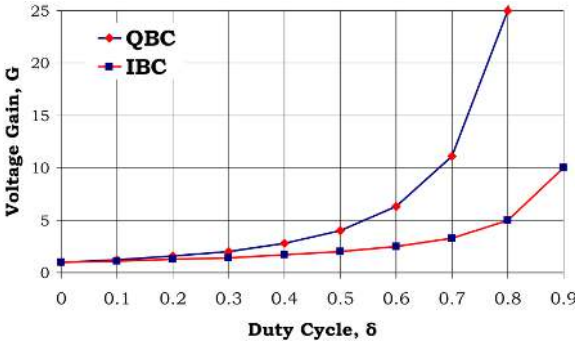

Fig. 13. Variation of voltage gain between QBC and IBC for various duty cycles

By applying amp–sec balance at C, the current flowing through L_1 (I_{L1}) and L_2 (I_{L2}) are obtained as

$$I_{L1} = I_{L2} = \frac{I_{out}}{2(1-\delta)} = \frac{V_{in}}{2(1-\delta)^2 R} \qquad \text{(Eq.29)}$$

The input is the sum of I_{L1} and I_{L2} and is obtained as

$$I_{in} = I_{L1} + I_{L2} = \frac{I_{out}}{(1-\delta)} = \frac{V_{in}}{(1-\delta)^2 R} \qquad \text{(Eq.30)}$$

The comparison of the input currents of QBC and IBC is depicted in Fig. 14. As the duty cycle increases, the input current of the QBC increases more predominately as compared with the IBC.

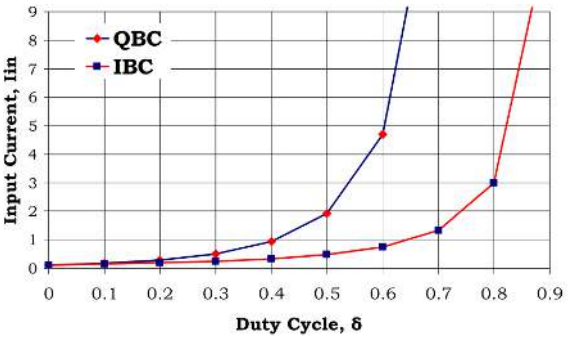

Fig. 14. Comparison of the input currents of QBC and IBC

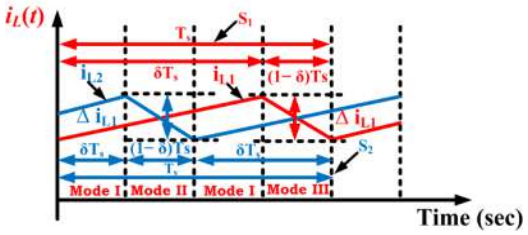

Fig. 15. Currents of L_1 and L_2 in IBC

The currents I_{L1} and I_{L2} are varying between maximum and minimum values a ripple of Δi_{L1} and Δi_{L2} respectively and are shown in the Fig. 15. The maximum ($I_{L1,\,max}$) and minimum ($I_{L1,\,min}$) currents of I_{L1} are obtained as

$$I_{L1,\max} = V_{in}\left[\frac{1}{2(1-\delta)^2 R} + \frac{\delta}{2L_1 f_S}\right] \qquad \text{(Eq.31)}$$

$$I_{L1,\min} = V_{in}\left[\frac{1}{2(1-\delta)^2 R} - \frac{\delta}{2L_1 f_S}\right] \qquad \text{(Eq.32)}$$

The maximum ($I_{L2,\,max}$) and minimum ($I_{L2,\,min}$) currents of I_{L2} are obtained as

$$I_{L2,\max} = V_{in}\left[\frac{1}{2(1-\delta)^2 R} + \frac{\delta}{2L_2 f_S}\right] \qquad \text{(Eq.33)}$$

$$I_{L2,\min} = V_{in}\left[\frac{1}{2(1-\delta)^2 R} - \frac{\delta}{2L_2 f_S}\right] \qquad \text{(Eq.34)}$$

Inductors L_1 and L_2 have the following critical values in IBC, and are

$$L_{1,cri} = \frac{\delta(1-\delta)^2 R}{f_S} \qquad \text{(Eq.35)}$$

$$L_{2,cri} = \frac{\delta(1-\delta)^2 R}{f_S} \qquad \text{(Eq.36)}$$

TABLE I summarises the comparison of QBC and IBC derived equations for the various parameter values.

TABLE I. Comparison of QBC and IBC derived equations for the various parameter values

S.No	Parameters	QBC	IBC
1.	Output Voltage, V_{out}	$\frac{V_{in}}{(1-\delta)^2}$	$\frac{V_{in}}{(1-\delta)}$
2.	Voltage Gain, G	$\frac{1}{(1-\delta)^2}$	$\frac{1}{(1-\delta)}$
3.	Input Current, I_{in}	$\frac{I_{out}}{(1-\delta)^2}$	$\frac{I_{out}}{(1-\delta)}$

4.	Inductor Currents	$I_{L1}=\frac{I_{out}}{(1-\delta)^2}$ $I_{L2}=\frac{I_{out}}{(1-\delta)}$	$I_{L1}=\frac{I_{out}}{2(1-\delta)}$ $I_{L2}=\frac{I_{out}}{2(1-\delta)}$
5.	Critical inductances	$L_{1,cri}=\frac{(1-\delta)^4\delta R}{2f_s}$ $L_{2,cri}=\frac{(1-\delta)^2\delta R}{2f_s}$	$L_{1,cri}=\frac{\delta(1-\delta)^2 R}{f_s}$ $L_{2,cri}=\frac{\delta(1-\delta)^2}{f_s}$

IV. Results and Discussions

Simulations in MATLAB using the PLECS Block set are used to verify the theoretical studies. A MOSFET is considered a switch in QBC and IBC. Table 2 depicts the specifications used for QBC and IBC in simulation. Here the all the parameters for both QBC and IBC are same. For CCM, the inductance values are considered more than their critical values. The input voltage is considered as 12 V, which is low voltage generated by the renewable energy sources.

TABLE II. Specifications of QBC and IBC for simulation

S.No.	Parameter	Value	
		QBC	IBC
1.	Input Voltage, V	12	12
2.	Duty Cycle, δ	0.6	0.6
3.	Switching Frequency, Hz	100 kHz	100 kHz
4.	Inductances, μH	L_1=L_2= 300 μH	L_1=L_2= 300 μH
5.	Capacitances, μF	C_1=C_2=10 μF	C=10 μF
6.	Load resistance , Ω	100 Ω	100 Ω

Switching pulses along the input current of QBC and IBC are indicated in Fig. 16 (a) and (b) respectively. The input current for QBC is 4.69 A and 0.75 A for IBC. The input current ripple in QBC and IBC is 0.24 and 0.08 respectively.

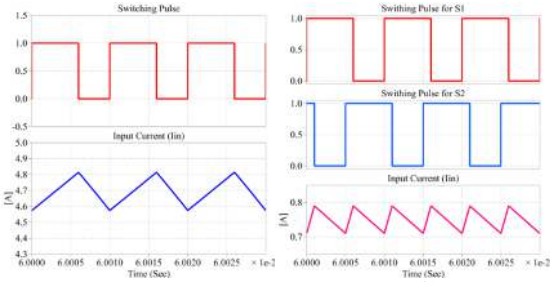

(a) (b)

Fig. 16. Switching pulses and input current of (a) QBC and (b) IBC

The output current and voltage of QBC and IBC are depicted in the Fig. 17 (a) and (b) respectively. For δ= 0.6, the output current and voltage of QBC are 0.7 A and 75 V, respectively, while for IBC they are 0.3 A and 30 V.

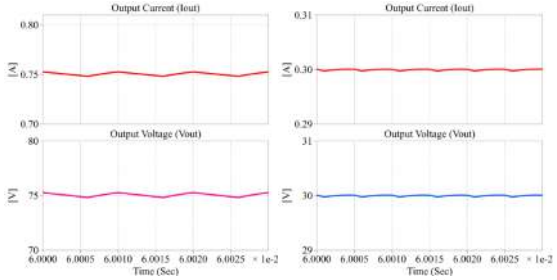

(a) (b)

Fig. 17. Output current and voltage for (a) QBC and (b) IBC

Fig. 18(a) and (b) show the current and voltage of the inductors in QBC. The current flowing through L_1 is equal to the input current, and the current flowing through L_2 is 1.88 A. The voltage across L_1 is equal to 12 V when charging and 18 V when discharging. In L_2, it is 30 V and 45 V, respectively.

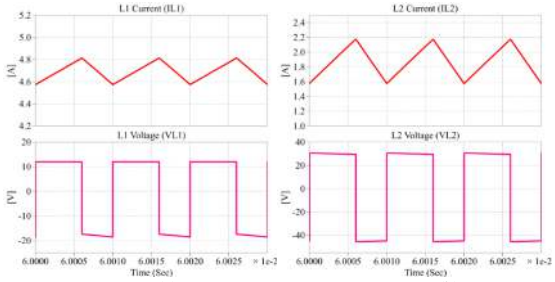

(a) (b)

Fig. 18. Inductors current and voltage of QBC (a) L_1 and (b) L_2

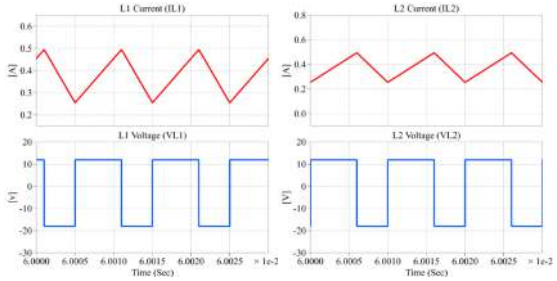

(a) (b)

Fig. 19. Inductors current and voltage of IBC (a) L_1 and (b) L_2

Fig. 19 (a) and (b) depict the IBC's inductors current and voltage. The input current is equally shared between L_1 and L_2. L_1 has a charging voltage of 12 V and a discharging voltage of 18 V. In the same way, L_2 is the same.

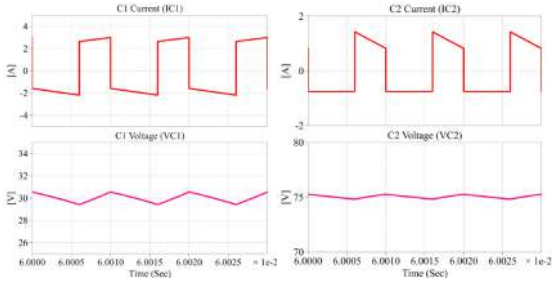

(a) (b)

Fig. 20. Capacitors current and voltage of QBC (a) C_1 and (b) C_2

Fig. 20(a) and (b) show the current and voltage of the capacitors in the QBC. The currents flowing through C_1 and C_2 are the currents of L_2 and I_{out}, respectively. The voltage across C_1 is equal to 30 V and C_2 is 75 V, which is the same V_{out} in QBC. The capacitor current and voltage of the IBC are indicated in Fig. 21. The inductors' current charges the capacitor C, which then discharges a steady load current. Its voltage is precisely the same as that of output voltage. It can be seen that there is less of a ripple in the current and voltage of the IBC than there is in the capacitors of the QBC.

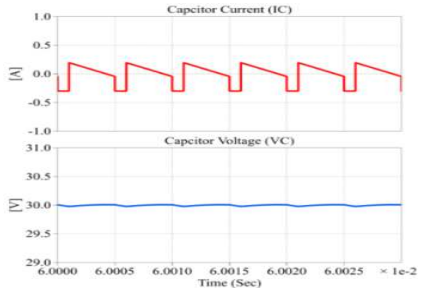

Fig. 21. Capacitor current and voltage of IBC

Fig. 22 depicts the current and voltage stresses in the power semiconductor devices (D_1, D_2, D_3, and S) of QBC. The currents of D_1 and D_2 are equal to I_{L1} of QBC, whereas the current of D_3 is I_{L2}. The current of S is the sum of I_{L1} and I_{L2}. D_1, D_2, D_3, and S have voltage stresses of 30 V, 45 V, 75 V, and 75 V, respectively. The current and voltage stresses in the power semiconductor devices (D_1, D_2, S_1 and S_2) of the IBC are shown in Fig. 23. The current and voltage stress of D_1 and D_2 are I_{L1} and V_{out}. Similarly, the switches S_1 and S_2 have the same current and voltage stresses.

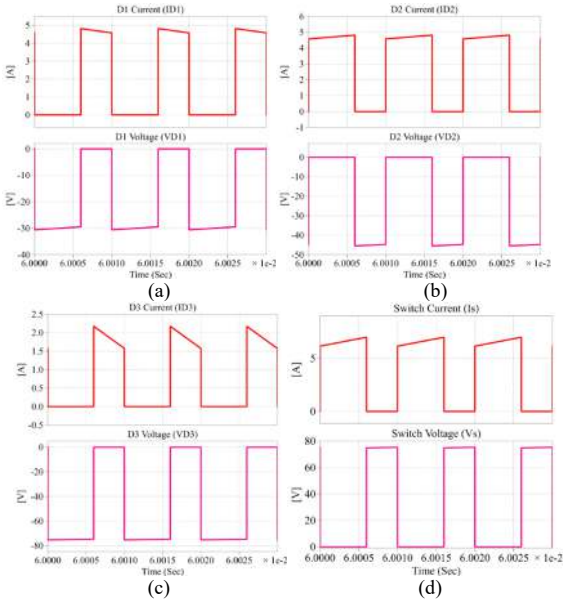

Fig. 22 Current and voltages stress of power semiconductor devices in QBC (a) D_1, (b) D_2, (c) D_3 and (d) S

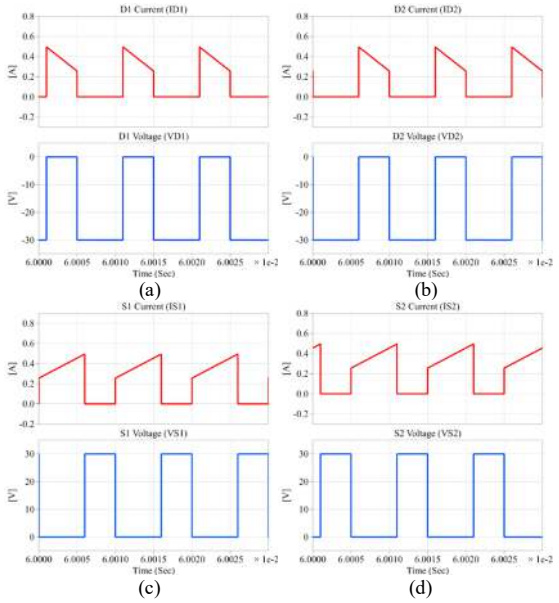

Fig. 23 Current and voltages stress of power semiconductor devices in IBC (a) D_1, (b) D_2, (c) S_1 and (d) S_2

The various parameter values of QBC and IBC are compared and shown in Table 3 for the specifications in Table 2. For the same duty cycle, the QBC provides 2.5 times the voltage as compared with the IBC. IBC draws 6.2 times less input current than QBC and input current is distributed evenly across inductors. The input current ripple in IBC is less than QBC. When compared to IBC, the current and voltage stresses of power semiconductor devices in QBC are significantly higher.

TABLE III. Comparison between QBC and IBC for various parameters values

S. No	Parameters	QBC	IBC
1.	Duty Cycle (δ)	0.6	0.6
2.	Input Voltage (Vin), V	12	12
3.	Input current (I_{in}), A	4.69	0.75
4.	Input Current ripple (Δi_{in}), A	0.24	0.08
5.	Inductor current(I_L), A	I_{L1}=4.69, I_{L2}=1.88	I_{L1}=0.375, I_{L2}=0.375
6.	Inductor current ripple(Δi_L), A	Δi_{L1}=0.24, Δi_{L2}=0.6	Δi_{L1}=0.24, Δi_{L2}=0.24
7.	Output Voltage(V_{out}), V	75	30
8.	Output Current (I_{out}), A	0.75	0.3
9.	Voltage Gain (G)	6.25	2.5
10.	Voltage stress on Switch (V_S), V	75	V_{S1}=30, V_{S2}=30
11.	Voltage stress on Diode (V_D), V	V_{D1}=30, V_{D2}=45 ,	V_{D1}=30, V_{D2}=30

		V_{D3}=75	
12.	Current stress on Switch (I_S), A	6.57	I_{S1}=0.375, I_{S2}=0.375
13.	Current stress on Diode (I_D), A	I_{D1}=4.69, I_{D2}=4.69, I_{D3}=1.88	I_{D1}=0.375, I_{D2}=0.375

The components used in QBC and IBC are indicated in Table 4. Both the QBC and the IBC make use of the same amount of input voltage sources and inductors. In QBC, one capacitor and a diode are used as compared with IBC. One extra switch is used in the IBC.

Table IV. Comparison of BC and QBC components

S. No.	Name of the Component	No. of Components	
		QBC	IBC
1	DC source	1	1
2	Inductor	2	2
3	Switch	1	2
4	Capacitor	2	1
5	Diode	3	2

V. CONCLUSION

This paper's primary goal is to compare the two converters. The two converters are analysed in a steady state with the ideal values. Expressions are developed for output voltage, voltage gain, inductor current, and ripple. Evaluated the equations for the design of inductors. The QBC has a larger voltage gain than the IBC for a given duty ratio. As opposed to QBC, the input current ripple in IBC is less. The current drawn from the source is higher in QBC than in IBC. In QBC and IBC, the voltage stress of the switches is equal to their respective output voltages. QBC is used in renewable energy applications where significant voltage gain is needed, while IBC is preferable when the input current ripple is specific to a low value.

REFERENCES

[1] Forouzesh, M., Siwakoti, Y.P., Gorji, S.A., Blaabjerg, F. and Lehman, B., 2017. Step-up DC–DC converters: a comprehensive review of voltage-boosting techniques, topologies, and applications. IEEE transactions on power electronics, 32(12), pp.9143-9178.

[2] Chou, T.H., Lin, W.C., Lee, Y.S. and Yu, L.C., 2014, October. An interleaved high gain boost converter for high power PV system applications. In TENCON 2014-2014 IEEE Region 10 Conference (pp. 1-7). IEEE.

[3] Changchien, S.K., Liang, T.J., Chen, J.F. and Yang, L.S., 2009. Novel high step-up DC–DC converter for fuel cell energy conversion system. IEEE Transactions on Industrial Electronics, 57(6), pp.2007-2017.

[4] Li, W., Lv, X., Deng, Y., Liu, J. and He, X., 2009, February. A review of non-isolated high step-up DC/DC converters in renewable energy applications. In 2009 Twenty-Fourth Annual IEEE Applied Power Electronics Conference and Exposition, pp. 364-369.

[5] N. Mohan, T. M. Undeland, W. P. Robbins, 2010. Power Electronics: Converters, Applications and Design. 3rd Ed. John Willey& Sons, India. ISBN: 9788126510900, pp- 172- 173.

[6] Philip T. Krein, 2003. Elements of Power Electronics. Oxford University Press, ISBN: 9780199388417, pp-384-386.

[7] R. W. Erickson and D. Maksimovic, 2001. Fundamentals of Power Electronics," Kluwer Academic Publishers, ISBN: 9781461576464, pp.805-812.

[8] D. W. Hart, 2011. Introduction to Power Electronics, Mc. graw Hill, India. ISBN: 9780071321204, pp. 211-220.

[9] Jain, S. and Agarwal, V., 2007. A single-stage grid connected inverter topology for solar PV systems with maximum power point tracking. IEEE transactions on power electronics, 22(5), pp.1928-1940.

[10] Angalaeswari, S., 2021. Design and execution of Quadratic Boost Converter (QBC) in Renewabe Energy Synergies. Turkish Journal of Computer and Mathematics Education (TURCOMAT), 12(9), pp.2957-2968.

[11] Morales-Saldana, J.A., Galarza-Quirino, R., Leyva-Ramos, J., Carbajal-Gutierrez, E.E. and Ortiz-Lopez, M.G., 2007. Multiloop controller design for a quadratic boost converter. IET Electric Power Applications, 1(3), pp.362-367.

[12] Ortiz-Lopez, M.G., Leyva-Ramos, J., Diaz-Saldierna, L.H., Garcia-Ibarra, J.M. and Carbajal-Gutierrez, E.E., 2007, June. Current-mode control for a quadratic boost converter with a single switch. In 2007 IEEE Power Electronics Specialists Conference, pp. 2652-2657.

[13] S Zhang, S., Xu, J. and Yang, P., 2012, December. A single-switch high gain quadratic boost converter based on voltage-lift-technique. In 2012 10th International Power & Energy Conference (IPEC), pp. 71-75.

[14] Nahar, S. and Uddin, M.B., 2018, September. Analysis the performance of interleaved boost converter. In 2018 4th International Conference on Electrical Engineering and Information & Communication Technology (iCEEiCT), pp. 547-551.

[15] Newlin, D.J.S., Ramalakshmi, R. and Rajasekaran, S., 2013, March. A performance comparison of interleaved boost converter and conventional boost converter for renewable energy application. In 2013 International Conference on Green High Performance Computing (ICGHPC), pp. 1-6.

[16] Lee, P.W., Lee, Y.S., Cheng, D.K. and Liu, X.C., 2000. Steady-state analysis of an interleaved boost converter with coupled inductors. IEEE transactions on industrial electronics, 47(4), pp.787-795.

[17] Selvaraju, N., Shanmugham, P. and Somkun, S., 2017. Two-phase interleaved boost converter using coupled inductor for fuel cell applications. Energy Procedia, 138, pp.199-204.

[18] Alzahrani, A., Ferdowsi, M. and Shamsi, P., 2019. A family of scalable non-isolated interleaved DC-DC boost converters with voltage multiplier cells. IEEE Access, 7, pp.11707-11721.

[19] Fekri, M., Molavi, N., Adib, E. and Farzanehfard, H., 2017. High voltage gain interleaved DC–DC converter with minimum current ripple. IET power electronics, 10(14), pp.1924-1931.

[20] O'Loughlin, M., 2007. An interleaved PFC preregulator for high-power converters. In Topic 5: Texas Instrument Power Supply Design Seminar , pp. 5-1.

[21] Axelrod, B., Beck, Y. and Berkovich, Y., 2015. High step-up DC–DC converter based on the switched-coupled-inductor boost converter and diode-capacitor multiplier: steady state and dynamics. IET Power Electronics, 8(8), pp.1420-1428.

[22] Prabhala, V.A.K., Fajri, P., Gouribhatla, V.S.P., Baddipadiga, B.P. and Ferdowsi, M., 2015. A DC–DC converter with high voltage gain and two input boost stages. IEEE Transactions on Power Electronics, 31(6), pp.4206-4215.